PB89-206718

Evidence for Cloud Venting of Mixed Layer Ozone and Aerosols

(U.S.) Environmental Protection Agency, Research Triangle Park, NC

1988

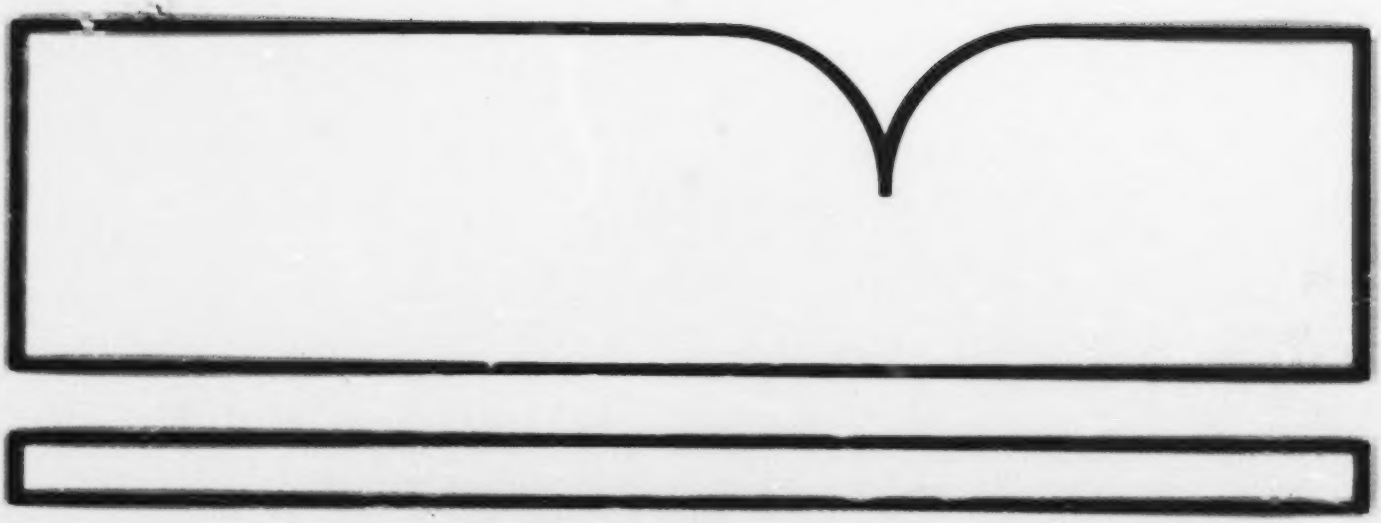

U.S. Department of Commerce
National Technical Information Service
NTIS

TECHNICAL REPORT DATA (Please read Instructions on the reverse before complet)		
1. REPORT NO. EPA/600/J-88/327	2.	3. PB89-206718
4. TITLE AND SUBTITLE EVIDENCE FOR CLOUD VENTING OF MIXED LAYER OZONE		5. REPORT DATE 6. PERFORMING ORGANIZATION CODE
7. AUTHOR(S) J.K.S. Ching, S.T. Shipley, and E.V. Browell		8. PERFORMING ORGANIZATION REPORT NO.
9. PERFORMING ORGANIZATION NAME AND ADDRESS J.K.S. Ching, ASRL, US EPA, RTP, NC 27711; S.T. Shipley and E.V. Browell, NASA, LRC, Hampton, VA 23665		10. PROGRAM ELEMENT NO. A101/B/63/21 - 1324 (FY-87) 11. CONTRACT/GRANT NO.
12. SPONSORING AGENCY NAME AND ADDRESS Atmospheric Sciences Research Laboratory--RTP, NC, Office of Research and Development, U. S. Environmental Protection Agency, Research Triangle Park, NC 27711		13. TYPE OF REPORT AND PERIOD COVERED 14. SPONSORING AGENCY CODE EPA/600/09
15. SUPPLEMENTARY NOTES Atmospheric Environment, Vo. 22, No. 2, pp. 225-242, 1988		

16. ABSTRACT

Observations are presented which substantiate the hypothesis that significant vertical exchange of ozone and aerosol pollutants occurs between the mixed layer and the free troposphere during cumulus cloud convective activity. Flight experiments conducted in July 1981, utilized the airborne UV-DIAL (Ultra-Violet Differential Absorption Lidar) system developed by NASA. This system provides simultaneous range resolved ozone concentration and aerosol backscatter profiles with high spatial resolution. Data were obtained during the afternoon along East to West and South to North intersecting transects over North Carolina in the presence of active, non-precipitating cumulus clouds. Evening transects were obtained in the downwind area of the sampled air mass. Space-height cross section analyses for the evening flight show the cloud "debris" as patterns of aerosol and ozone in excess of the ambient free tropospheric background. The ozone excess was approximately the value of the concentration difference between the afternoon mixed layer and free troposphere measured in the afternoon from independent in-situ vertical soundings made by another aircraft.

17. KEY WORDS AND DOCUMENT ANALYSIS		
a. DESCRIPTORS	b. IDENTIFIERS/OPEN ENDED TERMS	c. COSATI Field/Group

18. DISTRIBUTION STATEMENT	19. SECURITY CLASS (This Report)	21. NO. OF PAGES
RELEASE TO PUBLIC	UNCLASSIFIED	20
	20. SECURITY CLASS (This page) UNCLASSIFIED	22. PRICE MF A02 13.95/106.95

EPA Form 2220-1 (Rev. 4-77) PREVIOUS EDITION IS OBSOLETE

EPA/600/J-88/327

Atmospheric Environment Vol. 22, No. 2, pp. 225–242, 1988.
Printed in Great Britain.

0004–6981/88 $3.00 + 0.00
Pergamon Journals Ltd.

EVIDENCE FOR CLOUD VENTING OF MIXED LAYER OZONE AND AEROSOLS

J. K. S. CHING*

U.S. Environmental Protection Agency, Atmospheric Sciences Research Laboratory, Research Triangle Park, NC 27711, U.S.A.

S. T. SHIPLEY† and E. V. BROWELL

National Aeronautics and Space Administration, Langley Research Center, Hampton, VA 23665, U.S.A.

(*First received* 24 *November* 1986 *and in final form* 30 *June* 1987)

Abstract—Observations are presented which substantiate the hypothesis that significant vertical exchange of ozone (O_3) and aerosol pollutants occurs between the mixed layer and the free troposphere during cumulus cloud convective activity. Flight experiments conducted in July 1981 utilized the airborne UV-DIAL (Ultra-Violet Differential Absorption Lidar) system developed by NASA. This system provides simultaneous range resolved O_3 concentration and aerosol backscatter profiles with high spatial resolution. Data were obtained during the afternoon along east–west and south–north intersecting transects over North Carolina in the presence of active, non-precipitating cumulus clouds. Evening transects were obtained in the area indicated by trajectory calculations to be the current position of the air mass sampled earlier in the day. Space–height cross-section analyses for the evening flight show the cloud 'debris' as patterns of aerosol and O_3 in excess of the ambient free tropospheric background. The O_3 excess was approximately the value of the concentration difference between the afternoon mixed layer and free troposphere measured in the afternoon from independent *in-situ* vertical soundings made by another aircraft.

Key word index: Vertical exchange, cloud venting, pollutant transport, ozone transport, cloud transport, UV-DIAL, convective cloud transport.

1. INTRODUCTION

Cumulus clouds have the potential to transport pollutants from the mixed layer into the overlying free troposphere. Cloud activity, therefore, may be an important factor in controlling the chemistry, air quality and climate on regional and global scales. For example, observational studies of vertical transport of mixed-layer pollutants by precipitating convective clouds have been documented recently for thunderstorms (Dickerson *et al.*, 1987) and for mesoscale convective storms (Lyons *et al.*, 1986). In addition to such systems there is a class of cumulus which are of the non-precipitating type. The vertical exchange of moisture by such clouds have been well documented for the case of trade wind cumuli, e.g. Riehl (1979). Scorer (1978) has also suggested that pollutants should be carried upwards by such clouds. Theoretical model results by Gidel (1983) suggest that convective clouds can play an important role in vertical transport of pollutants. Currently, regional scale air pollution models for airborne pollutants such as oxidants (Lamb, 1982) and acids (Chang, 1985) now incorporate the linkage and exchange processes which occur between the mixed layer and the overlying free troposphere by cumulus convection (Vukovich and Ching, 1985; Ritter, 1983, 1984).

Given the recent attention on cloud processes and its importance to air quality models, it is important to review the bases and evidence for vertical transport by clouds. Figure 1 illustrates schematically the processes which are believed to occur during convective cloud activity. During periods of strong insolation, vigorous rising thermals can evolve into cumulus clouds which carry mixed-layer air with its pollutant burden within its updrafts. A large number of these clouds remain within the mixed layer and are defined as 'forced' clouds by Stull (1985). More buoyant clouds, however, can penetrate the mixed layer top inversion and 'vent' their contents into the free troposphere. Stull defines these clouds as 'active'. Both forced and active clouds are characteristically short lived, with time scales < 1 h. As active clouds lose their buoyancy, they become 'passive' clouds and eventually evaporate, leaving mixed layer pollutant debris trapped aloft above the mixed layer. The terms 'forced', 'active' and 'passive' as used hereinafter will follow these concepts. The net vertical transport depends both on the vertical and areal extent of the active convective clouds as well as on the pollutant concentration differences between the mixed layer and the overlying free troposphere. Pollutants which are entrained into these clouds

*On assignment from the National Oceanic and Atmospheric Administration, U.S. Department of Commerce.

†Currently with ST Systems Corp., Lanham, MD 20706, U.S.A.

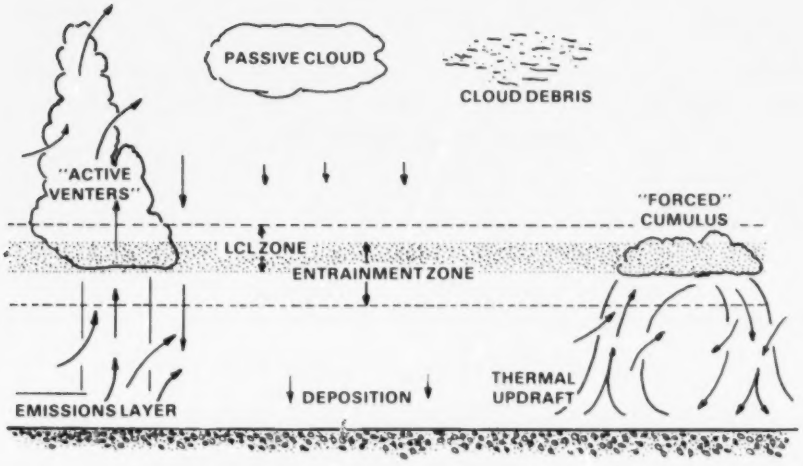

Fig. 1. Schematic of cloud activity for forced, active and passive cumulus clouds. Following Stull (1985), active clouds achieve a net transport of mixed layer tracers into the free troposphere after penetrating the mixed layer top inversion. The stippled area represents the overlap between the entrainment and lifting condensation level (LCL) zones.

undergo heterogeneous transformation processes (Alkezweeny and Hales, 1981; Hegg and Hobbs, 1982). While aloft, these pollutants are transported along paths different from those in the mixed layer below, and they therefore impact different receptors when they are re-entrained into the mixed layer (Shipley *et al.*, 1984; Uthe *et al.*, 1985).

Recent experiments by Alkezweeny and Hales (1981), Ching (1982), Ching *et al.* (1983), Ching and Alkezweeny (1985, 1986), Liu *et al.* (1984) and Greenhut *et al.* (1984) provide limited observations that infer vertical pollutant transport into the free troposphere occurs by venting clouds. However, the 'proof of principle' for a net deposition by non-precipitating clouds has yet to be substantiated. For example, it is conceivable that the downdrafts associated with the evaporating clouds carry with it all of the pollutants from within the original updraft back into the mixed layer. In this situation, the net transport is zero. Strong downdrafts associated with non-precipitating cloud fields have been observed to reach the surface by Ching *et al.* (1986), but it was not determined whether such air parcels were originally from cloud environment or from the evaporating cloud elements. Obviously, it is important to provide evidence that net pollutant exchange does take place due to cumulus activity. This paper describes an experiment which was conducted during July 1981, using the National Aeronautics and Space Administration (NASA) airborne UV-DIAL system (see below) which was designed to provide such observational evidence. A preliminary discussion of this effort was presented by Ching *et al.* (1984).

2. EQUIPMENT

Since cloud activity is highly variable in time and space and the physical processes are so complex, experimental sampling strategies will require high spatial and temporal resolution measurements of the pollutant fields. Detailed horizontal and vertical cross-sections of O_3, aerosol and other pollutant tracers would provide suitable observational bases. Such measurements can now be obtained by utilizing airborne UV-DIAL (Ultra-Violet Differential Absorption Lidar) systems which are capable of providing remote and range resolved observations of O_3 and atmospheric aerosols (Browell *et al.*, 1983). The NASA UV-DIAL system utilizes two Nd:YAG lasers to optically pump two high conversion efficiency tunable dye lasers with outputs at 572 and 600 nm. These outputs are optically split; one part of each beam is then frequency doubled into the Hartley Ultra-Violet (UV) O_3 absorption band, one at 286 nm (on-line) and the other at 300 nm (off-line). These two beams and the remaining output at 600 nm are then directed into the atmosphere, and the backscattered return signals are collected by a telescope, detected by photomultiplier tubes, digitized, and stored on magnetic tape. Given no range variation in the optical backscatter cross-section due to aerosols, the logarithmic difference between the two backscattered signals in the UV is directly proportional to O_3 concentration. For spatially inhomogeneous aerosol distributions, an aerosol scattering correction for the O_3 concentration profile is calculated using simultaneous lidar information on aerosol scattering at UV and visible wavelengths (Browell *et*

al., 1985a). The UV-DIAL and data acquisition system provide range-resolved measurements of O_3 concentration profiles in real time. Additionally, the range-resolved aerosol backscatter is determined using the signal returns from the 600 nm wavelength beam. NASA has successfully developed, demonstrated and deployed an airborne UV-DIAL system onboard the NASA Electra aircraft in a number of field studies (Browell *et al.*, 1983, 1985b, 1987; Shipley *et al.*, 1984). Data for the cloud study presented in this paper were sampled at the rate of 5 profiles s^{-1} with a vertical resolution of 15 m for aerosol backscatter and 210 m for O_3. The maximum horizontal resolution at an average aircraft ground speed of 125 m s^{-1} is 25 m. Precision in the O_3 concentration measurement is increased by horizontal and/or vertical averaging, albeit at the loss of spatial resolution. The O_3 analyses presented here utilized a horizontal average over 25 lidar profiles corresponding to a nominal horizontal resolution of 625 m. The vertical range for which the UV-DIAL measurements of O_3 concentration can be made, which is the difference between the near and far field range, is in excess of 1 km. The beginning of the near field range is determined by the geometry of the lidar optical detection system and the need to avoid signal saturation due to high levels of scattered light. The far field range is determined by signal loss due to optical attenuation or the interception of the Earth's surface.

As shown by Browell *et al.* (1983, 1985a, b), comparison of the UV-DIAL O_3 profile with simultaneous *in-situ* measurements obtained on board a Cessna aircraft shows excellent agreement. Most *in-situ* O_3 profile intercomparison data were obtained during the 1980 PEPE/NEROS Summer Field Experiment (Vaughan *et al.*, 1982), using a Monitor Lab Model 8410A O_3 analyzer onboard a Cessna 402 (Gregory *et al.*, 1981). As shown in detail in Browell *et al.* (1985a), the UV-DIAL mean O_3 measurements generally agree with the *in-situ* measurements to within $\pm$ 10 ppbv for ambient concentrations of order 50 ppbv or greater, when both measurements are made at the same time and location. The UV-DIAL measurements display increasing uncertainty near the bottom of the measurement range (at far range or lower altitude), where the one standard deviation variability is on the order of 15 ppbv. UV-DIAL generated O_3 profiles show systematic biasing within 210 m of discontinuities in aerosol concentration, due to changes in the wavelength dependence of atmospheric backscattering at the on and off DIAL wavelengths. Therefore, an aerosol backscatter correction procedure was developed (Browell *et al.*, 1985a) which reduces the variation between UV-DIAL and Cessna O_3 profile observations to < 7 ppbv. Both measurement techniques show excellent agreement in the magnitude of small scale variations in O_3 concentration, indicating that UV-DIAL measurement of coincident O_3 and aerosol in cloud remnants can be used with confidence.

3. DESCRIPTION OF THE EXPERIMENT

A field experiment was designed to follow and characterize the pollutant distribution in an elevated air mass known to have contained some active type cumulus clouds. In this study, pollutants observed to be embedded in the layer above the top of the mixed layer inversion after cumulus activity ceased would be hypothesized to be the deposited remnants of dissipated clouds. The experiment was conducted using the NASA airborne UV-DIAL onboard the NASA Electra aircraft. The Electra flew two missions over North Carolina on 22 July 1981. The flight patterns are shown in Fig. 2. The first mission pattern consisted of an along-wind (east–west) leg starting at 1509 EDT (Eastern Daylight Time) with a cross-wind (south–north) transect starting at 1538 EDT. Both flight legs intersected over the Raleigh/Durham airport (35°52′N, 78°47′W) with each leg covering about 140 km. The evening mission used a similar flight pattern consisting of an along-wind leg of 110 km starting at 2129 EDT and a cross-wind leg of 130 km starting at 2201 EDT. This pattern was located over an area just west of the North Carolina coast which was the projected trajectory position of the same air mass sampled during the afternoon. This projected air mass trajectory was subsequently verified by isentropic analyses as shown below. An instrumented Cessna 402 twin engine aircraft provided concurrent vertical profiles of O_3, aerosol backscatter coefficient B_{scat}, temperature (T) and dew point (T_d) derived from sequential down and up ramp patterns along the same flight coordinates. This was accomplished for both the afternoon and evening Electra sampling periods. The Electra aircraft operational altitude was 4 km MSL. The Cessna vertical data profiles were obtained at altitudes from near surface to greater than 3 km MSL. The Cessna down ramp legs were A-X and C-X in the afternoon and both evening transects, while flight segments X-B and X-D were up ramp legs. GOES satellite data and routine NWS/NOAA ancillary surface and upper air weather observations were archived for subsequent data analysis.

4. RESULTS AND DISCUSSION

a. *Meteorological analyses*

Streamline analyses for airflow at relevant altitudes are shown in Fig. 3. A cold front oriented SW–NE passed over Central North Carolina at 0200 EDT on 22 July 1981, moved southeastward, and was along the North Carolina coastline at the time of the streamline analyses. The mixed layer winds over central North Carolina and northward into central Virginia were generally north–northwesterly, becoming more westerly with increasing altitude throughout the study period. Above the mixed layer, the west–northwest flow backed with height to westerly winds at 3000 m

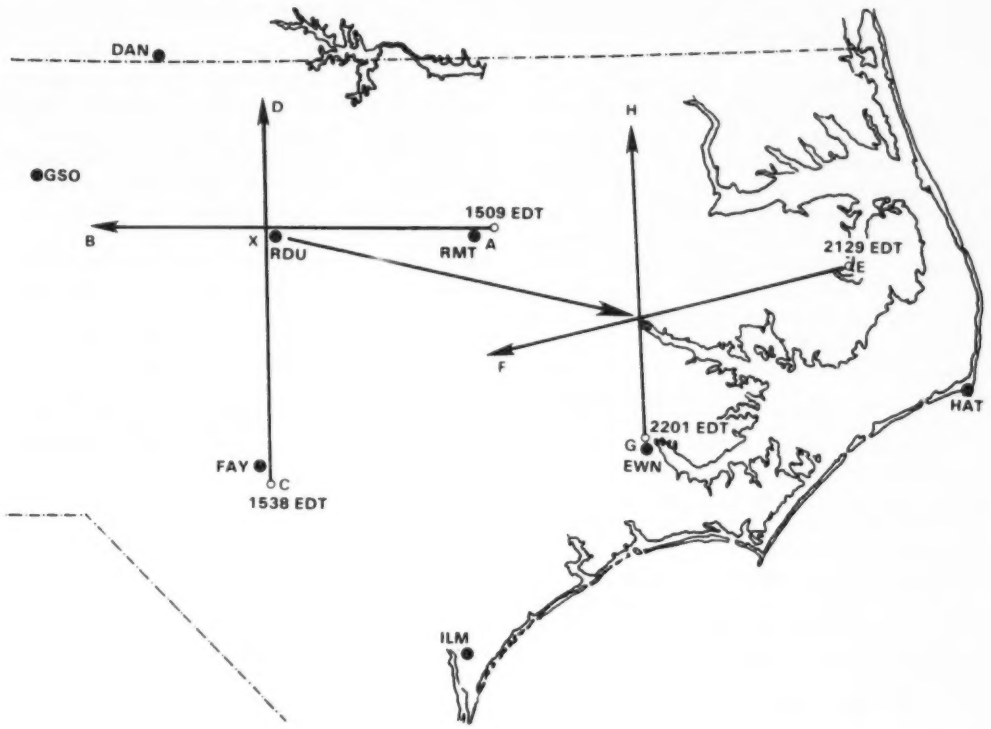

Fig. 2. Flight orientation of the Electra and Cessna aircraft for monitoring cloud convective activity. An afternoon sample was obtained flying east–west at 1509 EDT, and from south to north at 1538 EDT. The evening sample was obtained in the same air mass flying east–west at 2129 EDT and from south to north at 2201 EDT.

MSL (Mean Sea Level). The average wind speed shear was 2.5 $m\,s^{-1}\,km^{-1}$. The surface flow pattern suggests that the source region for pollutants vented by cumulus clouds over north central North Carolina may be due in part to urban emissions from the Richmond, Virginia area many hours earlier.

Table 1 lists relevant environmental parameters determined from the Cessna profile and surface data. Mixed layer heights were derived from the *in-situ* T, T_d, B_{scat} and O_3 measurements from each vertical profile. The mixed layer height was defined as that height where the largest change in the vertical gradient in parameter magnitude occurs. The mixed layer height for each parameter did not differ significantly from the composite group mean value. Moreover, the mixed layer heights did not vary appreciably among the different ramps. Height values shown in parentheses indicate the presence of a second layer. The lifting condensation level (LCL) and the limit of free convection (LFC) were also computed from the aircraft soundings. Note that the LCL height is higher than the mixed layer height. The computed LCL using Raleigh–Durham (RDU) National Weather Service surface hourly T and T_d observations was 1700 m and is about the same as the observed mixed layer height. However, even though the observed LCL is higher than the observed mixed layer height, the difference is smaller than the difference observed by Wilde *et al.* (1985) to support the development of cumulus clouds. Wilde explains that convective cumulus clouds can form even when the LCL is higher than the mixed layer by several hundreds of meters if the zones of LCLs and entrainment overlap significantly (Fig. 1).

GOES images show that non-precipitating, active type, cumulus clouds were prevalent and also highly variable in their spatial distribution and in time over the sampling domain from 1200 to 1700 EDT. Figure 4 shows five GOES satellite views of the cloud field during the experiment. The aircraft flight in the afternoon corresponded closely in time with the central figure. Prior to flight time the air mass did not experience cumulus development until afternoon. Shallow fair weather cumulus were embedded within the mixed layer and interspersed with the venting type clouds. At the time of the flight, cumulus cloud tops varied from 1.5 to 4 km AGL. Observers on board the Electra aircraft noted that several active clouds extended above the flight level of 4 km MSL during the afternoon. The cloud field became more organized in late afternoon (see 1730 EDT) and finally disappeared after 1930 EDT.

Figure 5 presents back trajectories of the cross

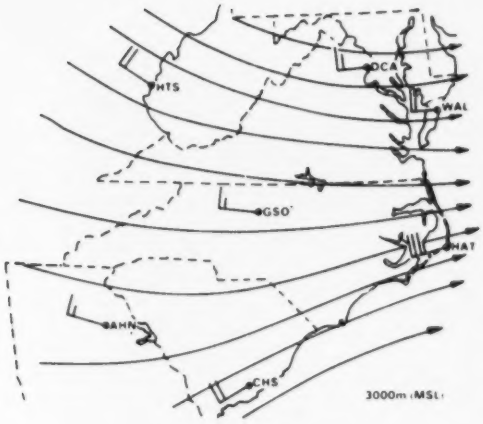

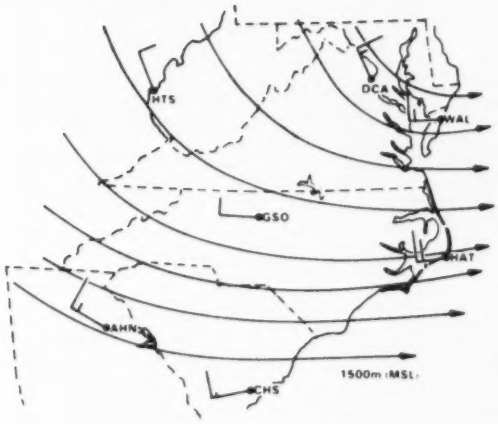

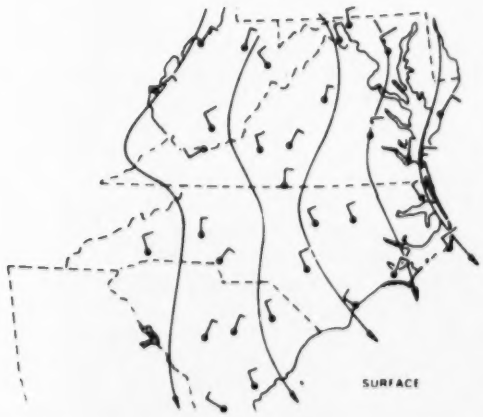

Fig. 3. Streamline analyses for mixed layer and free troposphere flow for 0800 EDT on 22 July 1981, at 3000 m MSL (a), 1500 m MSL (b) and near the surface (c).

Table 1. Environmental parameters from Cessna sounding data on afternoon of 22 July 1981

Flight leg	Mixed layer height (m MSL)	LCL* (m MSL)	LFC† (m MSL)
A-X	1680	1860	2630
X-B	1700 (1900)	1880	2530
C-X	1700	2000	2650
X-D	1690 (1430)	2100	2100
(High)	1900		
Mean	1690	1960 (1700)‡	2480
(Low)	1430		

*Lifting condensation level.
†Limit of free convection.
‡LCL (from RDU airport surface data).

pattern of the evening transect for three air mass layers in the altitude ranges from 1500 to 2000 m MSL, 2000 to 2500 m MSL and 2500 to 3000 m MSL. The back trajectories for the upper two layers were computed along isentropic surfaces, while the lowest layer was derived assuming isobaric flow. These trajectory analyses reflect the backing of the wind direction with altitude and the wind speed shear noted earlier. The second layer is closest in juxtaposition to the flight track of the afternoon mission.

b. *Aircraft soundings*

The afternoon soundings of T, T_d, O_3 and B_{scat} obtained by the Cessna aircraft are shown in Fig. 6 and they suggest a mixed layer height of 1560 m AGL. The lapse rate in the mixed layer was nearly adiabatic from the surface up to the base of the elevated inversion with stable thermal stratification aloft. T_d values decreased slightly with height within the mixed layer but decreased more rapidly with altitude aloft. *In-situ* B_{scat} and O_3 observations indicated large and variable concentrations in the mixed layer with generally lower concentrations in the free troposphere.

Distinct differences between the east–west and the south–north cross-sections were observed in the Cessna data. Along the east–west section, the O_3 and B_{scat} exhibited only small vertical gradients and relatively little variation in spatial structure. Mixed layer O_3 concentrations were generally about 70–80 ppb and decreased by little more than 10 ppb above the mixed layer. In contrast, the south–north cross-section exhibited large horizontal and vertical variations. Maximum O_3 values in the down ramp approach to RDU airport from the south were in excess of 100 ppbv. Much smaller concentrations in O_3 and B_{scat} were observed above 1700 m. Given the observed NNE mixed layer wind, these high values were possibly associated with the RDU urban plume. The mixed layer air quality structure observed in the upramp flight from RDU northward did not indicate a discernible urban plume and was generally similar to the east–west Cessna flight observations. Above the mixed layer, however, the O_3 and B_{scat} profiles indicated large

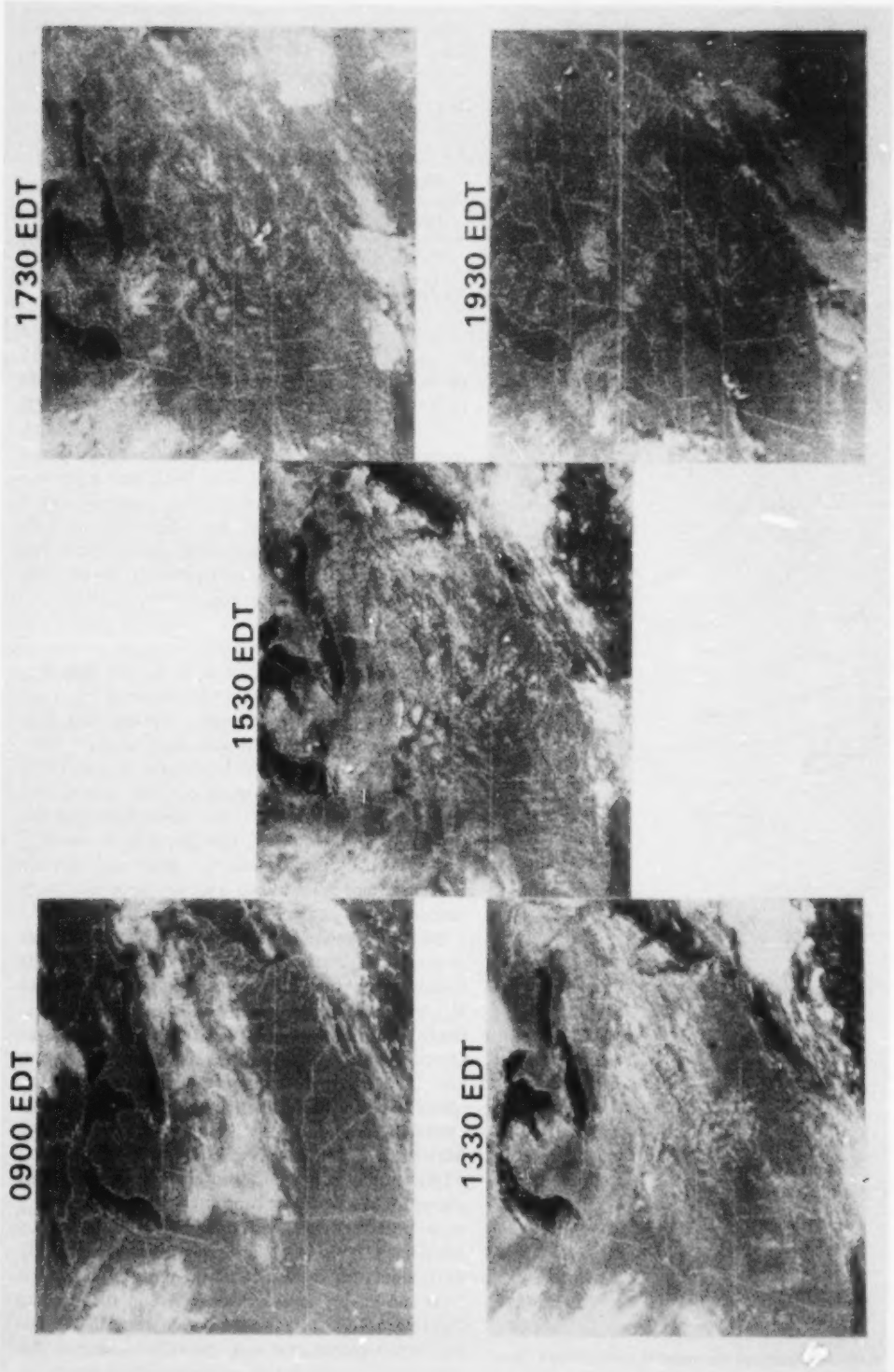

Fig. 4. GOES satellite images of cloud activity on 22 July 1981.

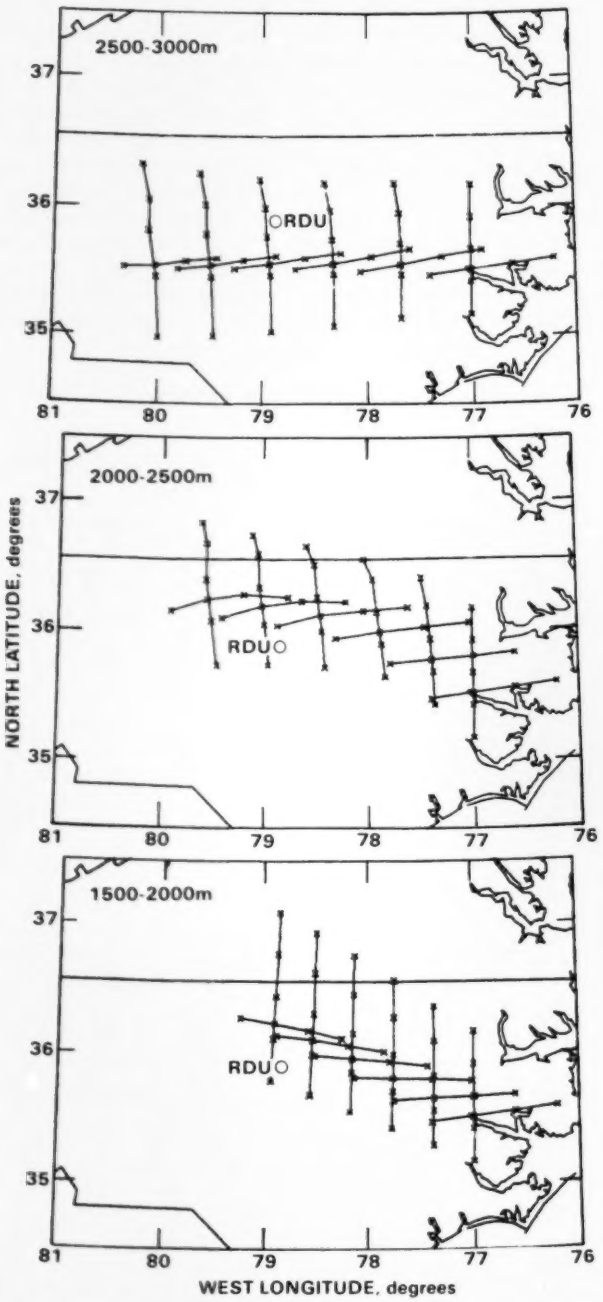

Fig. 5. Back trajectories at 2-h intervals of the cross-wind pattern for the evening transect (2200 EDT) of the Electra aircraft on 22 July 1981 for three air mass layers, (a) 1500–2000 m MSL (isobaric), (b) 2000–2500 m MSL (isentropic) and (c) 2500–3000 m MSL (isentropic).

values, comparable to those in the mixed layer. T_d was also higher in this inhomogeneous region compared to the other soundings. According to our calculations shown in Table 2 and Fig. 6, the convective cloud activity was relatively more pronounced in this area at the time of this observation as well as earlier in the upwind region.

As shown in Fig. 7, the determination of the top of

the mixed layer as the height where the gradients in T, moisture, O_3 and B_{scat} were largest is not unique when examining the Cessna flight data made in the evening. The evening Cessna data were obtained during a down ramp flight leg from east to west and also from a down ramp south to north leg along the same track taken by the UV-DIAL system. The east to west profile E-F suggests a mixed layer top either at 1200 m from the temperature and moisture data, at 1500 m using the B_{scat} data, and either at 1200 m or 1700 m using the O_3 observations. The data from the south to north ramp flight support 1200 m using B_{scat}, O_3 and T_d data, but perhaps 1500 m using T and also T_d observations. The lower value of about 1200 m is more consistent with isentropic flow calculations and kinematic calculations using the routine NWS upper air soundings (Ritter, 1983). The structure, however, suggests the presence of thin layers from different upwind air masses overlying each other due to wind shear. The air in the lowest kilometer is inferred to be from the Norfolk, Virginia area from streamline analyses of the wind field since the wind flow was generally northeasterly in the Virginia Tidewater area. However, due to the backing of wind with height, the layers aloft are from more westerly areas as indicated by the isentropic back trajectory analyses shown in Fig. 5. The O_3 concen-

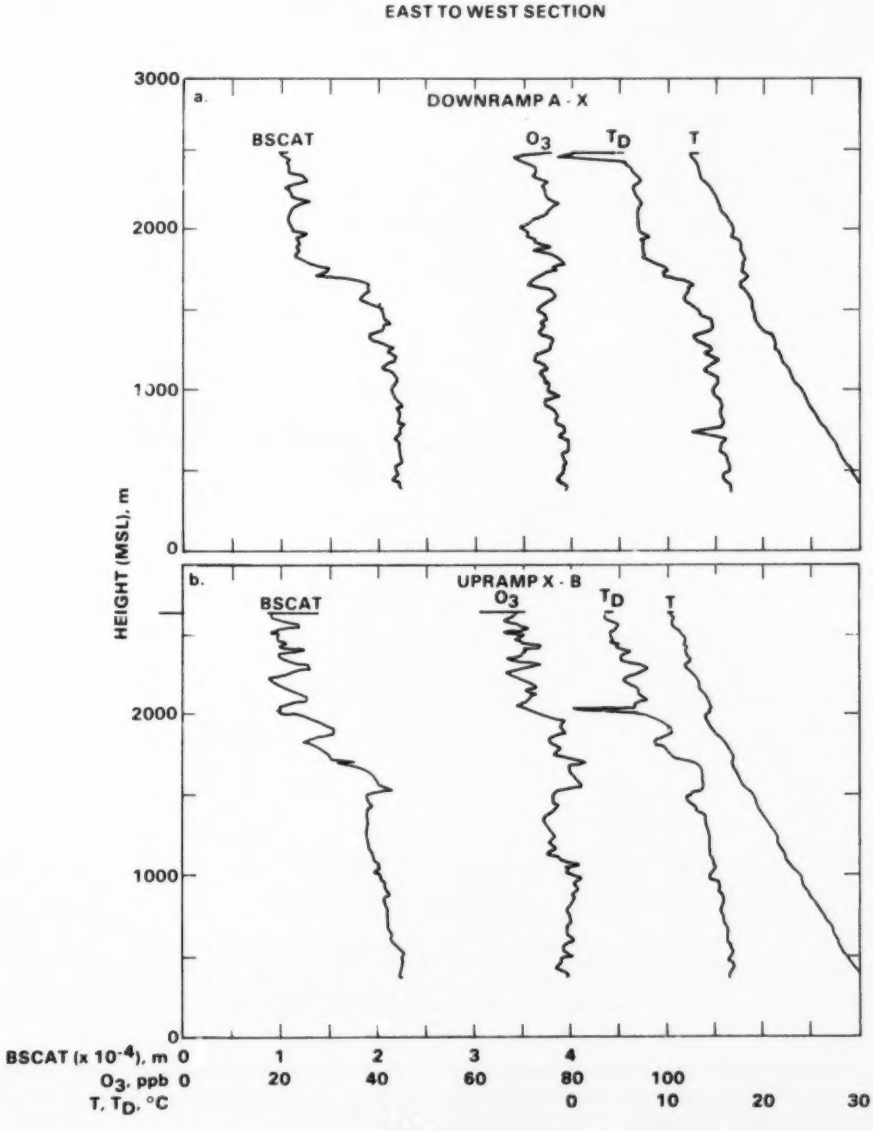

Fig. 6(a–b).

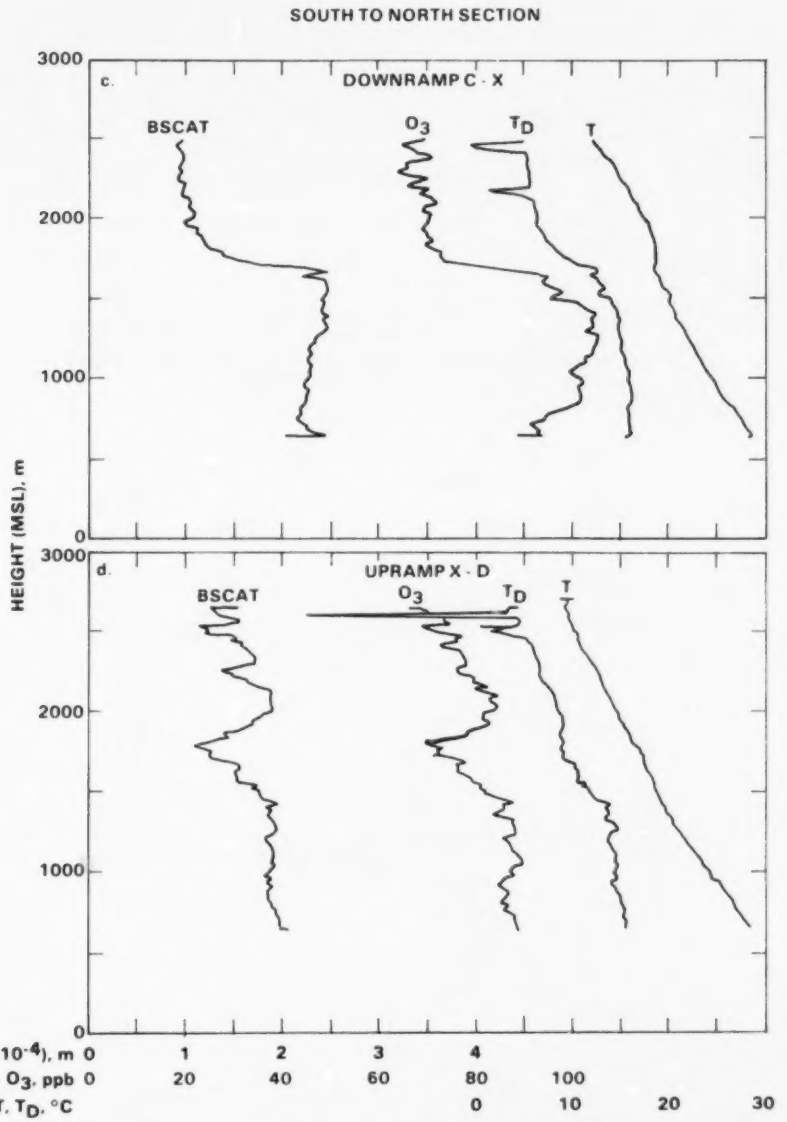

Fig. 6. Sounding data from Cessna flights made concurrently with the Electra flights in the afternoon on 22 July 1981. The data were taken from up and downramp profiling flights for (a) along-wind down (A-X) from 1509 EDT to 1524 EDT, (b) along-wind up (X-B) from 1524 EDT to 1545 EDT, (c) cross-wind down (C-X) from 1609 EDT to 1624 EDT, and (d) cross-wind up (X-T) from 1624 EDT to 1642 EDT.

trations in the lowest kilometer are in excess of 90 ppb and are suggestive of an urban plume from a large source area such as greater metropolitan Norfolk. B_{scat} values are about $4 \times 10^{-4}\ m^{-1}$.

c. Lidar cross-sections

Figures 8 and 9 show UV-DIAL observations of particulate cross-sections for the afternoon and evening missions, respectively. Backscatter returns for the east–west segment of the afternoon observation period are shown in Fig. 8a. The spatial pattern of the aerosol distribution is fairly homogeneous, both vertically and horizontally. The backscatter data of Fig. 8a indicate that the primary type of cumulus clouds present are those of the forced variety with several active clouds also present. The forced clouds are those which appear as dark regions embedded in or near the top of the mixed layer. An example of this type of cloud is indicated as C1 in Fig. 8a. The forced cloud C1 has sufficient optical depth to eliminate lidar return signals

Table 2. Average daytime percentage convective cloud cover in Lagrangian coordinates for the Electra south–north evening cross-section on 22 July 1981

South Height (MSL)	A/B*				North
3000	6/7*	12/10	17/14	25/21	28/23
2500	20/17	26/18	47/31	46/31	46/30
2000	9/14	26/20	38/31	31/24	35/28
1500					
Average	12/13	21/16	34/25	34/25	36/27

* Values in table show percentages computed for two averaging periods, A (1200–1800 EDT), B (1200–2200 EDT).

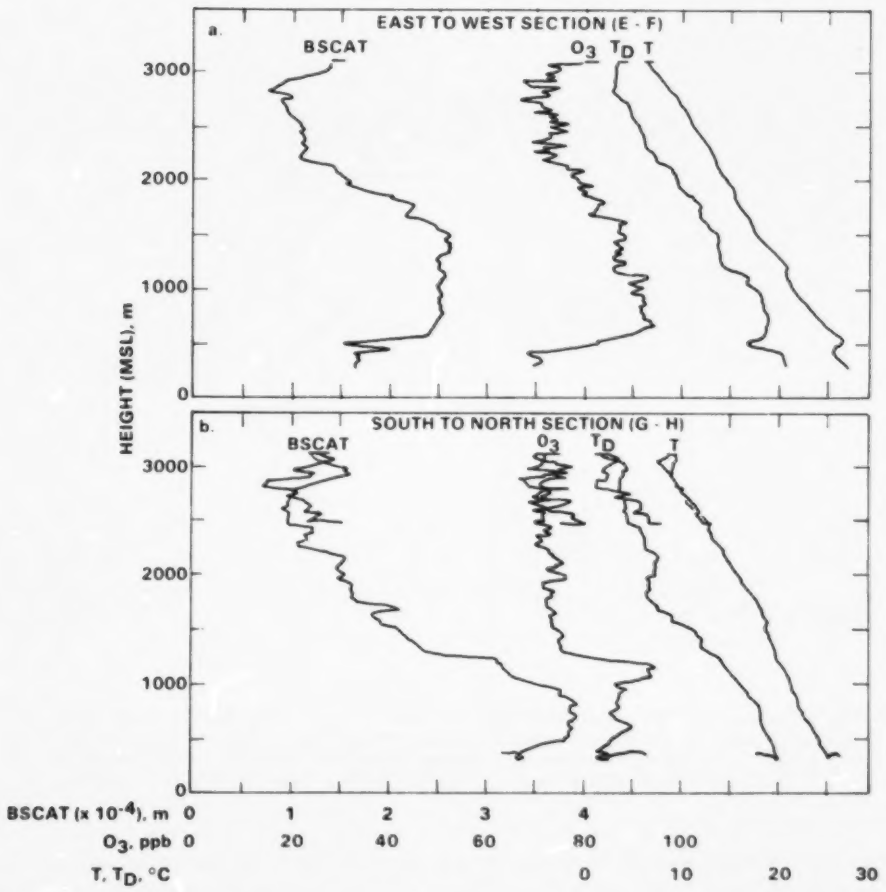

Fig. 7. Same as Fig. 6 except for evening flight (a) along-wind down (E-F), and (b) cross-wind down (G-H).

from aerosols and the ground surface below the initial cloud top boundary. Other forced clouds can be seen at lower altitudes that are optically thin. Single cloud element widths vary from 200 m to somewhat > 1 km. Active clouds are identified as those clouds whose tops protrude significantly above the top of the mixed layer. Feature C2 is an example of such a cloud which protruded to 2500 m AGL, about 700 m above the top of the adjacent mixed layer.

Passive type clouds are not readily discernible in this

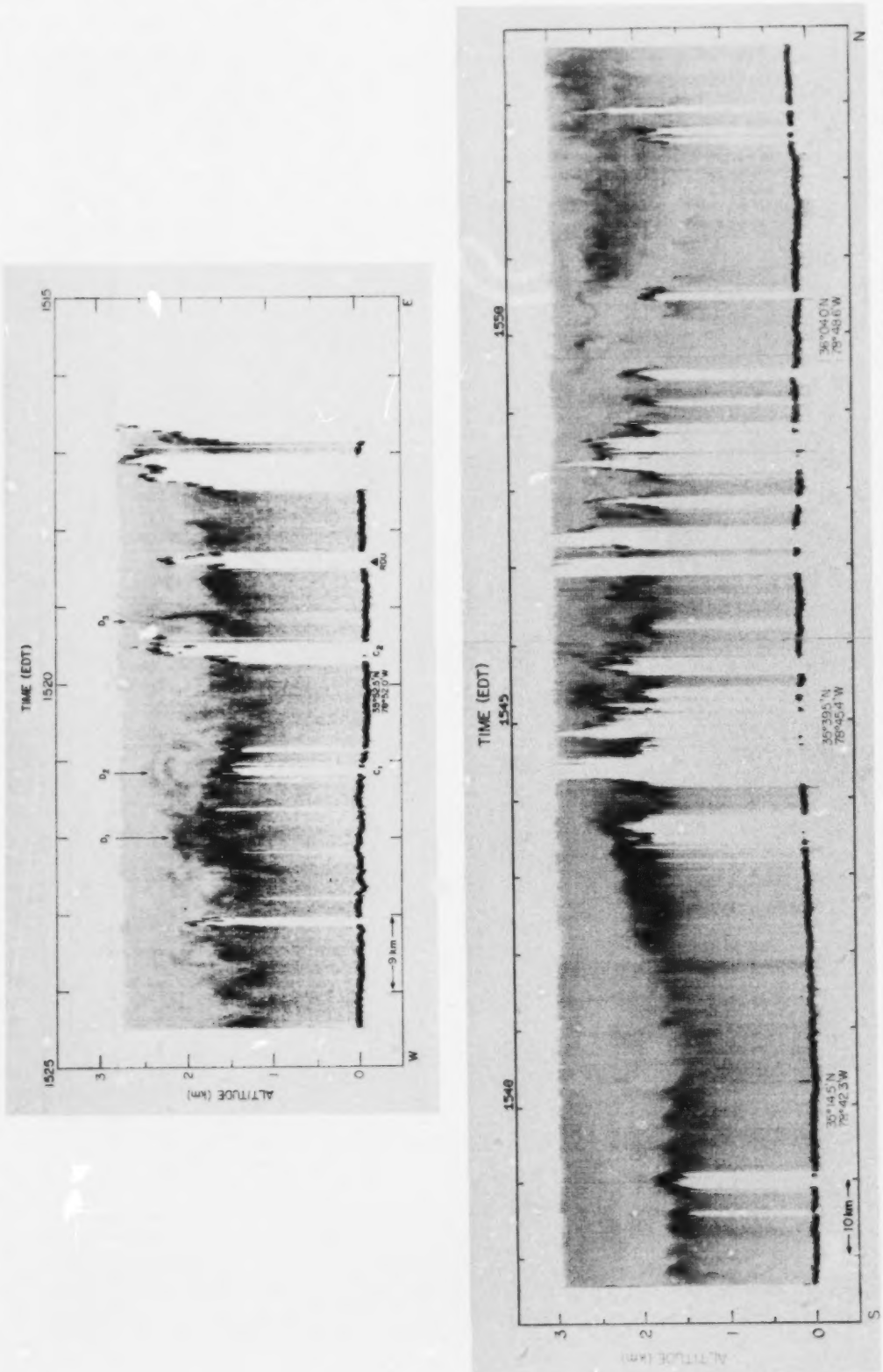

Fig. 8. Vertical cross-section of lidar aerosol backscatter data over central North Carolina from the Electra platform for the afternoon flight on 22 July 1981. (a) East–west and (b) south–north transect.

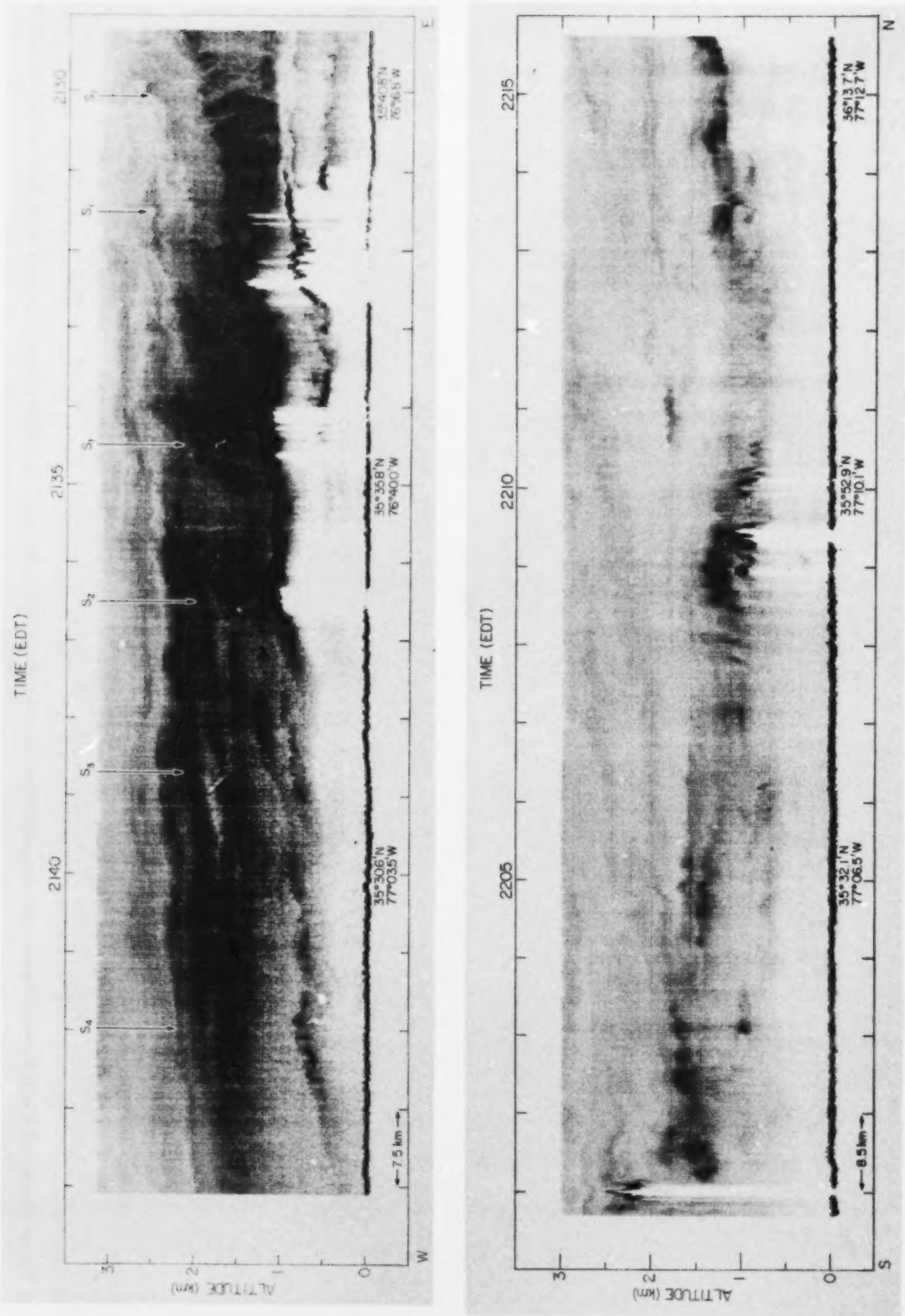

Fig. 9. Same as Fig. 8 but for the evening flight for (a) east–west and (b) south–north transects.

panel. However, the aerosol features D1, D2 and D3 are examples of possible decayed remnants of such clouds. D1 appears as a feature which is merely an extension of the vertical extent of the mixed layer. D2 is the decayed remnant of a passive cloud which has been injected into the relatively clean free troposphere above the mixed layer. D3 shows a passive cloud in the process of evaporating. The debris patches at the top of D3 are evaporated clouds, while the darker signal return below the top of this feature is a vertical column of relatively high opacity with little connection to the mixed layer. The mixed layer does exhibit some horizontal variations in depth. The range of this variation is greater than 500 m in this transect, and can be considered comparable to the entrainment zone thickness of a convective boundary layer.

Figure 8b shows the lidar backscatter cross-section for the south–north transect starting at 1538 EDT and crossing over the Raleigh–Durham airport. Active cumulus clouds (as well as some of the more optically thick forced-type clouds) which attenuate the lidar signal returns appear as white vertical columns. The mixed layer is clearly discernible in those areas where the cumulus convection was relatively light and scattered, as shown in the southern section at 1540 EDT. The haze is concentrated within the mixed layer, while lighter shadings at higher altitudes indicate relatively homogeneous spatial structure and low aerosol concentrations aloft. The top of the mixed layer increases with height to the north in the region where the concentration and development of convective cumulus clouds of the active type were relatively more pronounced. These convective elements literally cloud the issue of defining a mixed layer depth. The structure in the mixed layer and aloft in the northern portion of Fig. 8b from 1542 to 1554 EDT is very complex and consequently the mixed layer height is poorly defined. This air mass has had a recent history of convective cloud activity and it still contains numerous cumulus convective cloud elements. However, these clouds appear to be primarily those of the passive type as defined by Stull (1985). Consequently, the aerosol spatial distribution in the upper layers exhibits complex spatial structures which appear to be mixed layer pollutant debris. This presence of mixed layer debris is consistent with the Cessna aircraft observations from 1624 to 1642 EDT encountered from RDU northward, which characterized the zone of passive clouds (Fig. 6d).

Figure 9a shows the ENE–WSW cross-section of the backscatter signal return for the evening flight mission. The gray scale displays should not be used to infer absolute backscatter cross-sections. Each display panel has been adjusted to enhance the spatial patterns of the backscatter signal distribution. The character of this observation is totally different from that of the afternoon. With the exception of a few isolated clouds, the field of convective type cumulus clouds now appears as layers and patches of aerosol which are the evaporated remnants of the non-precipitating clouds. These layers slant upward in the vertical from west to east due to stronger winds at higher altitudes (Scorer, 1978). This vertical speed shear advects the upper portion of the cloud remnants a greater distance downwind relative to the lower part. Due to some wind direction shear, the flight leg only intersects portions of these tilted cloud remnants. The along-wind cross-section yields an average remnant slope or tilt of 16 m km^{-1} after a 6.5-h mean transport time, corresponding to an average vertical wind speed shear of about 2.5 m s^{-1} km^{-1}. Greater slopes would be attributable to the more recent clouds, while smaller slopes might be attributable to earlier cloud activity. For example, slopes for features indicated in Fig. 9a as S1, S2, S3 and S4 are 110, 30, 20 and 13 m km^{-1}, respectively, which correspond to transport times of 1, 4, 6 and 9 h prior to the time of this observation. It is interesting to note that all of these features exhibit the positive slope required for the given wind speed shear. Feature S1 is quite different in character from that of S2, S3 or S4. The length of S1 is considerably shorter, and the thickness is greater as would be expected for a passive cloud which has evaporated more recently.

The evening aerosol backscatter cross-section for the cross-wind flight leg is shown in Fig. 9b. The layered character of the cloud debris is similar to the extensive horizontal layering observed during the evening along wind flight. However, these layers exhibit both positive, zero and negative slopes with height. The cross-wind cloud remnants above 1000 m AGL predominantly slope to the north with altitude, indicating a wind direction shear 'backing' with height. This observation is in agreement with the air mass layer trajectories of Fig. 5.

Figures 10a and 10b show the along-wind (east–west) and cross-wind (south–north) O_3 concentration cross-sections, respectively, simultaneous to and coincident with the aerosol cross-sections of Figs 10a and 9b. The O_3 data extend vertically from 1300 to 2500 m AGL. Much of the fine detail which is seen in the aerosol gray scale displays has been spatially smoothed by horizontal and vertical O_3 averaging. The 60 ppb background O_3 concentration derived by UV-DIAL in this region is slightly lower than the background value determined from the Cessna observations. As shown in the UV-DIAL calibration studies discussed above, this difference should be viewed simply as a system bias and, therefore, the magnitude and position of the O_3 spatial patterns are not affected. O_3 concentrations > 70 ppb (10 ppb above background) are observed to be distributed in layers coincident with the aerosol layers with identical slopes due to wind shear. These positive O_3 excesses are comparable to the average O_3 concentration difference between the mixed layer and the cloud layer in the afternoon except for areas impacted by local sources such as urban and industrial plumes. As shown below, features associated with such plumes exhibit much larger concentration features. The O_3 distribution for both the along-wind and cross-wind analyses is limited

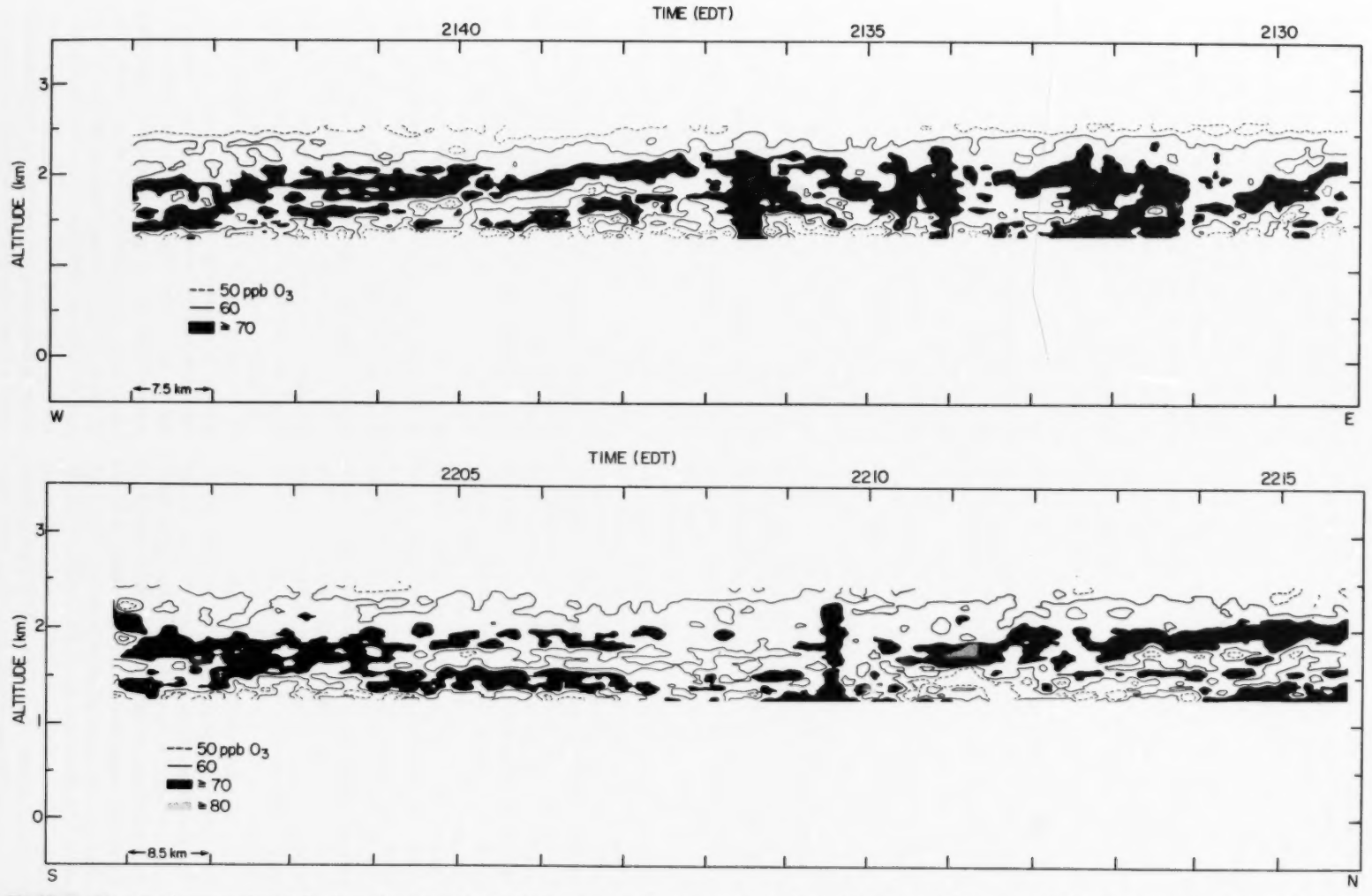

Fig. 10. Evening vertical cross-sections of O_3 observations from the UV-DIAL system simultaneous to and coincident with the aerosol cross-section of Fig. 9 for (a) east–west and (b) south–north transects. O_3 concentrations > 10 ppbv above the background value are indicated by the black shaded areas.

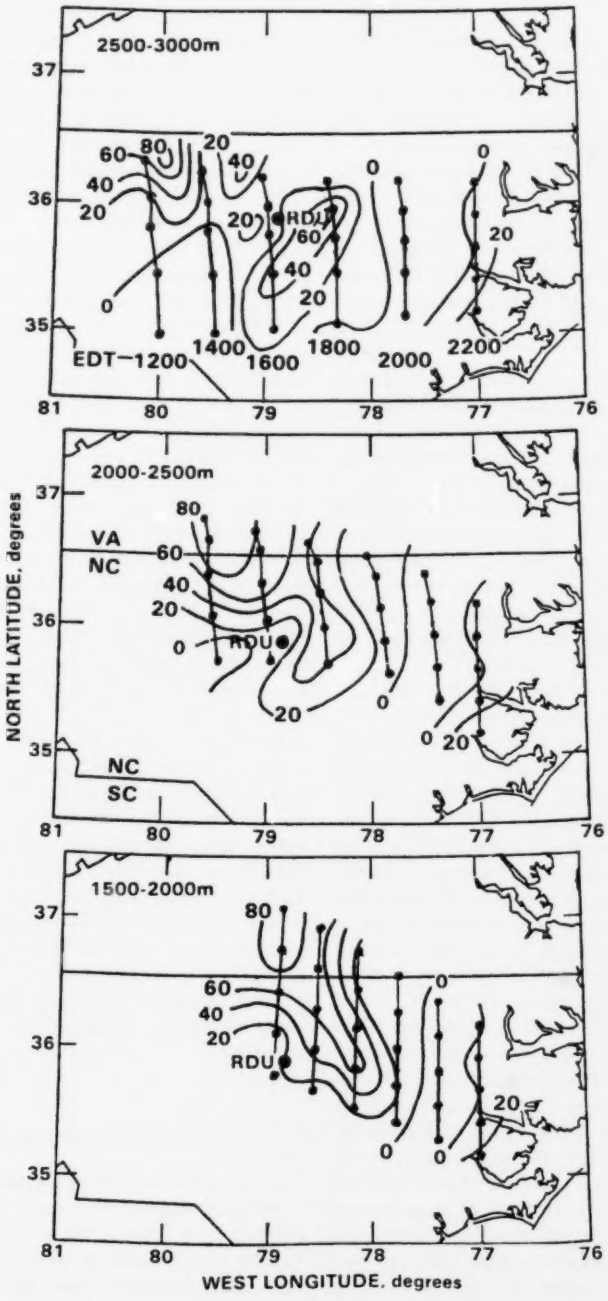

Fig. 11. Percentage areal coverage of cumulus cloud cover for 20 km × 20 km grids at 2-h intervals along the back trajectories of the cross-wind pattern shown in Fig. 5. These were data derived from digitized visible satellite imagery and represent cloud cover activity along a Lagrangian coordinate system associated with the evening transect of the Electra aircraft.

in vertical extent to about 2200 m AGL. In contrast, the maximum height of the active clouds observed in the afternoon extended to about 3000 m AGL. Isentropic flow analyses indicate that subsidence in the layer from the mixed layer top to about 700 mb was on the order of 2–3 cm s^{-1} which is sufficient to explain the lowering of the cloud debris layer by more than 500 m prior to the time of the evening mission.

The fractional cross-section area covered by positive O_3 anomalies defined as at least 10 ppbv over background in an air mass layer should be related to the areal coverage of clouds integrated over the period of time for which convective clouds were active in that air mass. The fractional area of the O_3 anomalies computed for the height interval from 1250 m to 2250 m AGL were found to be 25% and 30% for the along-wind and cross-wind transects, respectively. Values of percentage coverage varied from 40% for the southern most quarter section to 13% in the middle of the south–north transect. Thus, the areal coverage of the regions of positive O_3 anomalies is seen to be a significant percentage of the total cross-sectional area as monitored by UV-DIAL, and is also comparable to the percentage coverage of cloud activity during the preceeding 10 h. Note that this percentage will increase if the criteria for O_3 anomaly is reduced from 10 ppbv.

It should be stated that these vented products are not the result of isolated cumulus events, but represent the integration of many convective intrusions and subsequent injections of mixed layer aerosol and O_3 into the free troposphere throughout the afternoon. Since it is hypothesized that the pollutants vented into each of these layers is related to the amount of cloud debris left behind by cumulus clouds that previously penetrated into these layers, it is useful to provide information on the history of cloud activity in the moving air mass of each of these layers. For this study the spatial patterns of cloud cover as would be viewed on a coordinate system which moves with the mean wind in each of the layers are shown in Fig. 6. Back trajectories for each dot are shown in Fig. 11 at alternate hours from 2200 EDT back to 1200 EDT. These trajectory locations were then compared to the gridded cloud data. Hourly averaged values for convective cloud amount and cloud top height distribution were derived for 20 km square grids from the GOES data over the study domain (Behunek *et al.*, 1983). The areal percentage data on convective cloud cover were available as a function of altitude. The cloud amount data for the grids in closest proximity to each of the trajectory position at each bi-hourly time period were used to compute the percentage cloud cover available for venting to each air mass layer. The fractional area depicted is the value at the lowest altitude of each of the three 500 m layers. This figure indicates the time and duration of convective cloud activity during the air mass layer transport distributed along the south–north transect. The average convective cloud activity for the (A) 6 or (B) 10 h convective time period starting at 1200 EDT then is obtained by integrating this information in time along any portion of the segment and dividing by the transport period of convective activity. These results are shown in Table 2 for each of the 20 km flight segments and for each layer. The results indicate the total cloud activity was greater in the northern half of the flight section over the experiment period. Further, the cloud activity was, in general, greatest in the lower layers with a maximum in the 2000–2500 m layer, and much smaller cloud amounts above 2500 m.

Figure 12 presents a high resolution view of the relatively pronounced and compact feature observed during the south–north evening transect, in which the O_3 and the aerosol concentrations are significantly greater than those values observed within the mixed layer during the afternoon. O_3 concentrations > 90 ppbv (30 ppbv above background) were observed in this feature. A back trajectory analysis shows that this feature is coincident with the location of a large power plant located in Roxboro, NC. Plume rise computed for this power plant effluent was found to be less than the height of the mixed layer at the time the air mass was over the plant. The height of this feature was much higher than can be explained by simple dry convection, or as part of a deeper entrainment zone. However, it was well within the zone where active clouds were present. Although speculative, a plausible explanation for this feature is that power plant pollutants were caught in the updraft of an active cumulus convective cell and deposited aloft. However, in typical coal fired power plant plumes, the near source O_3 concentrations are generally lower than its background due to the NO emissions, but after several hours of photochemical activity, the O_3 concentrations do increase to large values. This can happen only if sufficient non-methane hydrocarbons from the mixed layer environment are also entrained with the plume into the cloud updrafts (Gillani and Wilson, 1980; Gillani *et al.*, 1981). The positive O_3 anomaly thus observed might be explained as a result of photochemical activity subsequent to its deposition in the cloud layer.

5. SUMMARY AND CONCLUSION

An airborne UV-DIAL system was utilized in a 'proof of principle' experiment designed to provide evidence of cloud venting of mixed layer pollutants (e.g. O_3 and aerosols) to the free troposphere. In this case study, the observations displayed O_3 pollutant concentration values in the layer above the convective mixed layer in excess of its background by the amount of the O_3 concentration difference between the mixed and cloud layers, as hypothesized. The O_3 profile data to determine the mixed layer–cloud layer concentration differences were obtained *in-situ* by another instrumented aircraft. The UV-DIAL observation

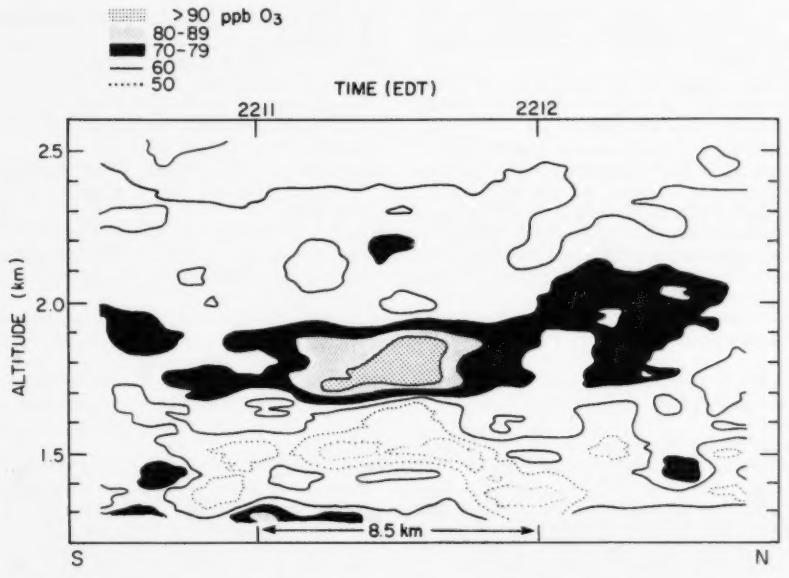

Fig. 12. Fine resolution vertical cross-section of O_3 from the UV-DIAL showing cross-wind observations for an elevated power plant plume located above the mixed layer.

showed the vented pollutants in the free troposphere to exhibit a layered structure.

Acknowledgements—The authors would like to express sincere appreciation to Syed Ismail for processing the lidar observational data, to David McDougal for coordinating the various platforms utilized in the field missions, and for reducing and processing the Cessna data. John Ritter provided the back trajectory computations, the cloud field analyses and many stimulating discussions. The technical support of C. Butler, A. Carter, M. Mayo, W. McCabe, N. McRae and L. Overbay of the DIAL group, and to S. Grice, C. Hudgins, G. Maddrea, Jr and G. Gregory with the Cessna operations is gratefully acknowledged. The first author gratefully acknowledges the NASA Langley Research Center for the invitation to participate in this study, and their subsequent support of a portion of the data analysis effort.

Disclaimer—Although the research described in this article has been partially supported by the United States Environmental Protection Agency, it has not been subject to Agency review and therefore does not necessarily reflect the views of the Agency and no official endorsement should be inferred.

REFERENCES

Alkezweeny A. and Hales J. M. (1981) The impact of nonprecipitating clouds on the transport and formation of acid aerosols. Annual Meeting American Chemical Society, New York.

Browell E. V., Carter A. F., Shipley S. T., Allen R. J., Butler C. F., Siviter M. N., Jr and Hall W. M. (1983) NASA multipurpose airborne DIAL system and measurements of ozone and aerosol profiles. *Appl. Optics* **22,** 522–534.

Browell E. V., Danielsen E. F., Ismail S., Gregory G. L. and Beck S. M. (1987) Tropopause fold structure determined from airborne lidar and *in situ* measurements. *J. geophys. Res.* **92,** 2112–2120.

Browell E. V., Ismail S. and Shipley S. T. (1985a) Ultraviolet DIAL measurements of O_3 profiles in regions of spatially inhomogeneous aerosols. *Appl. Optics* **24,** 2827–2836.

Browell E. V., Shipley S. T., Butler C. F. and Ismail S. (1985b) Airborne lidar measurements of aerosols, mixed layer heights and ozone during the 1980 PEPE/NEROS summer field experiment. NASA RP 1143.

Behunek J. L., Vonder Haar T. H. and Laybe P. (1983) Determination of cloud parameters for NEROS II from digital satellite data. EPA-600/3-84-044.

Chang J. (1985) NCAR Eulerian Regional Acid Deposition Model, NCAR/TN-256 + STR.

Ching J. K. S. (1982) The role of convective clouds in venting ozone from the mixed layer. Third Joint Conf. Appl. Air Pollut. Meteorol. San Antonio, TX. Preprint volume AMS, Boston, MA.

Ching J. K. S. and Alkezweeny A. J. (1985) Vertical transport by cumulus clouds. Preprint Vol., *7th AMS Symp. on Turbulence and Diffusion*, Boulder, CO, pp. 63–66.

Ching J. K. S. and Alkezweeny A. J. (1986) Tracer study of vertical exchange by cumulus clouds. *J. Clim. appl. Met.* **25,** 1702–1711.

Ching J. K. S., Clarke J. F., Irwin J. S. and Godowitch J. M. (1983) Relevance of mixed layer scaling for daytime dispersion based on RAPS and other field programs. *Atmospheric Environment* **17,** 854–871.

Ching J. K. S., Shipley S. T., Browell E. V. and Brewer D. (1984) Cumulus cloud venting of mixed layer ozone. *Proc. Quadrennial Ozone Conf.*, Sept, Halkidiki, Greece.

Dickerson R. R., Huffman G. J., Luke W. T., Nunnermacker L. J., Pickering K. E., Leslie A. C. D., Lindsey C. G., Slinn W. G. N., Kelly T. J., Daum P. H., Delany A. C., Greenberg J. P., Zimmerman P. R., Boatman J. F., Ray J. D. and Stedman D. H. (1987) Thunderstorms: an important mechanism in the transport of air pollutants. *Science* **235,** 460–465.

Gidel L. T. (1983) Cumulus cloud transport of transient tracers. *J. geophys. Res.* **88,** 6587–6599.

Gillani N. V., Kohli S. and Wilson W. E. (1981) Gas to particle conversion of sulfur in power plant plumes—I.

Parameterization of the conversion rates for dry, moderately polluted ambient conditions. *Atmospheric Environment* **15**, 2293–2314.

Gillani N. V. and Wilson W. E. (1980) Formation and transport of ozone and aerosols in power plant plumes. *Annals NY Acad Sci.* **338**, 276–296.

Greenhut G. K., Ching J. K. S., Pearson R., Jr and Repoff P. (1984) Transport of ozone by turbulence and clouds in an urban boundary layer. *J. geophys. Res.* **89**, 4757–4766.

Gregory G. L., Beck S. M. and Mathis J. J., Jr (1981) *In situ* correlative measurements for the ultraviolet differential absorption lidar and the high spectral resolution lidar air-quality remote sensors: 1980 PEPE/NEROS program. NASA TM-83107.

Hegg D. A. and Hobbs P. V. (1982) Measurements of sulfate production in natural clouds. *Atmospheric Environment* **16**, 2663–2668.

Lamb R. J. (1983) A regional scale (1000 km) model of photochemical air pollution—1. Theoretical formulation. EPA-600/3-83-035.

Liu S. C., McAfee J. R. and Cicerone R. J. (1984) Radon 222 and tropospheric vertical transport. *J. geophys. Res.* **89**, 7291–7297.

Lyons W. A., Calby R. H. and Keen C. S. (1986) The impact of mesoscale conventive systems on regional visibility and oxidants distributions during persistent elevated pollution episodes. *J. Clim. appl. Met.* **25**, 1518–1531.

Riehl H. (1979) *Climate and Weather in the Tropics.* Academic Press, London.

Ritter J. A. (1983) The vertical redistribution of a pollutant tracer due to cumulus convection. Ph.D. dissertation, Univ. of Michigan.

Ritter J. A. (1984) The determination of cloud base mass flux and the vertical redistribution of a conservative tracer. Transactions APCA Specialty Conf: *The Meteorology of Acid Deposition* (edited by Sampson P. J.), 16–19 Oct. Hartford, CN.

Scorer R. S. (1978) *Environmental Aerodynamics.* Ellis Horwood, Halstead Press, Division of John Wiley, New York.

Shipley S. T., Browell E. V., McDougal D. S., Orndorff B. L. and Haagenson P. (1984) Airborne lidar observations of long range transport in the free troposphere. *Environ. Sci. and Techn.* **18**, 749–756.

Stull R. B. (1985) A fair weather cumulus cloud classification scheme for mixed layer studies. *J. Clim. appl. Met.* **24**, 41–56.

Uthe E. E., Viezee W., Morley B. M. and Ching J. K. S. (1985) Airborne lidar tracking of fluorescent tracers for atmospheric transport and diffusion studies. *Bull. Am. met. Soc.* **66**, 1255–1262.

Vaughan W. W., Chan M., Cantrell B. and Pooler F. (1982) A study of persistent elevated pollution episodes in the United States. *Bull. Am. met. Soc.* **63**, 258–266.

Vukovich F. M. and Ching J. K. S. (1985) Modeling transport by convective clouds for regional air pollution models. Preprint Vol., *7th AMS Symp. on Turbulence and Diffusion*, Boulder, CO, 12–15 Nov., pp. 3–6.

Wilde N. P., Stull R. B. and Eloranta E. W. (1985) The LCL zone and cumulus onset. *J. Clim. appl. Met.* **24**, 640–657.

NOTICE

This document has been reviewed in accordance with U.S. Environmental Protection Agency policy and approved for publication. Mention of trade names or commercial products does not constitute endorsement or recommendation for use.

This article documents research that was conducted under the auspices of the U.S. Environmental Protection Agency (USEPA). As an arm of the government, the USEPA has a paid up, non-exclusive, irrevocable, worldwide license to reproduce, prepare derivative works, and distribute to the public all of the material contained herein, and to grant others acting on its behalf the right to do so. The USEPA grants to the National Technical Information Service, Department of Commerce, the right to act as its agent in the distribution of this material.